Polymers **2012**, *4*, 1399-1415; doi:10.3390/polym4031399

OPEN ACCESS

polymers

ISSN 2073-4360

www.mdpi.com/journal/polymers

Article

A Systematic Study on the Self-Assembly Behaviour of Multi Component Fmoc-Amino Acid-Poly(oxazoline) Systems

Pier-Francesco Caponi [1,*] and Rein V. Ulijn [2,*]

[1] Laboratory of Organic and Macromolecular Chemistry (IOMC), Friedrich-Schiller-University Jena, Jena 07745, Germany

[2] WestCHEM/Department of Pure and Applied Chemistry, University of Strathclyde, Glasgow G11XL, UK

***** Authors to whom correspondence should be addressed;
E-Mails: pier-francesco.caponi@uni-jena.de (P.F.C.); rein.ulijn@strath.ac.uk (R.V.U.);
Tel.: +49-3641-948294 (P.F.C.); +44-141-548-2110 (R.V.U.);
Fax: +49-3641-948202 (P.F.C.); +44-141-548-4822 (R.V.U.).

Received: 9 May 2012; in revised form: 6 July 2012 / Accepted: 10 July 2012 / Published: 24 July 2012

Abstract: We report a systematic study of a modular approach to create multi-component supramolecular nanostructures that can be tailored to be both enzyme and temperature responsive. Using a straightforward synthetic approach we functionalised a thermal responsive polymer, poly(2-isopropyl-2-oxazoline), with fluorenylmethoxycarbonyl-amino acids that drive the self-assembly. Depending on the properties of appended amino acids, these polymers undergo substantial morphological changes in response to the catalytic action of alkaline phosphatase.

Keywords: responsive polymers; amino acids; enzyme responsive materials

1. Introduction

Producing synthetic mimics of the adaptive compartmental systems of biological systems, through conformational changes under constant conditions, is a goal that has not been achieved [1–3]. This objective is often pursued through the use of polymers, whose properties and characteristics can be precisely tailored; often relying on a change in environmental conditions, e.g., change in ionic strength or pH value, to undergo morphological changes [4]. The use of enzyme responsive materials, has

attracted significant interest due to their capacity to operate under constant environmental conditions, *i.e.*, a change in conditions is not required to activate their catalytic activity. Moreover, the advantages of using enzyme for their catalytic action are well known, e.g., they operate under physiological conditions, they display inherent signal amplification and are biologically relevant and compatible, making these systems particularly appealing for biomedical applications [5,6].

Among the structures that can be formed by enzyme-responsive materials, micelle-like nanostructures are of particular interest due to the possibility to encapsulate drugs in the hydrophobic core [7] that could be released in a specific tissue, where the target enzyme is over-expressed. The control over the size and chemical composition of structures formed is a key issue, especially if the aim is to develop systems that can have applications in the drug delivery field. A strategy that can be used to obtain enzyme-responsive materials that self-assemble into colloidal aggregates, as reported by Hawker and co-workers [8] and by Kühnle and Börner [9], exploits diblock co-polymers which are hydrophilic but turn into amphiphilic upon enzymatic catalysis via dephosphorylation, leading to self-assembly. Also Gianneschi *et al.* [10] exploited an amphiphile copolymer to enable enzymatically triggered aggregation. In their work, a polymer was functionalised with peptides substrates for phosphatases, kinases and matrix metalloproteinases, achieving different morphological changes, such as transition from micelles to networks or micelles to amorphous aggregates, depending on the enzyme used. An alternative strategy, which involves the use of a non-covalent "super"-amphiphile, has been reported by Zhang and co-workers [11]. In this case, a diblock co-polymer is used which bears positive charges [poly(ethylene glycol)-poly(lysine)] [PEG-poly(K)] and, upon addition of negatively charged adenosine triphosphate (ATP), the system undergoes self-assembly due to ionic interactions between ATP and poly(K). Upon phosphatise-catalysed hydrolysis, the negatively charged molecules are digested, resulting in loss of the amphiphilic structure and dis-assembly. This strategy shows dis-assembly upon enzyme catalysis, which may be of interest for drug delivery purposes. The examples cited highlighted clearly demonstrate how molecular design of the non-covalent interactions within the system (in particulary electrosatics and hydrophobic interactions) can affect the self-assembly process.

We recently reported a system of phosphatase-responsive colloidal aggregates, composed of poly(2-isopropyl-2-oxazoline) (PiPrOx), a thermal responsive polymer, functionalised through a one-step synthetic strategy with fluorenylmethoxyloxycarbonyl-phosphorylated tyrosine [12], which is known to self assemble upon dephosphorylation [13]. Upon phosphatase catalysed hydrolysis, the functionalised polymers were found to self assemble forming micelles. Moreover, the system retained the reversible thermal properties typical of PiPrOx, *i.e.*, phase separation above the lower critical solution temperature (LCST). By introducing a second, cationic, component (Fmoc-K functionalised PiPrOx), a first example of a dual-component system was demonstrated. Rather than triggering the assembly of disassembly of aggregates, this system focused on reconfiguration from one self-assembled state to another [14].

Cooperative multicomponent systems provide an attractive means of introducing complexity into a system without increasing the complexity of the building blocks. By mixing different populations of functionalized PiPrOx polymers, it may be possible to exploit the interactions that can occur between these amino acids (in particular ionic and aromatic interactions). In here, we build upon our previous work and aim systematically study the influence of amino acid chemical structure on selfassembly

properties of PiPrOx. While our previously focused communications focused on the enzyme responsiveness [12] and ability to produce multi-component structures based on charge complementarity [14], we herein focus on the cooperative behaviour in multicomponent systems by studying the relative importance of aromatic and electrostatic interactions within one- and two component systems. We functionalised PiPrOx with amino acids bearing different characteristics: Fmoc-phosphorylated tyrosine (Fmoc-*p*Y) (negative), Fmoc-lysine (Fmoc-K) (positive), Fmoc-tyrosine (Fmoc-Y) and Fmoc-phenylanine (Fmoc-F) (hydrophobic and aromatic) amino acids.

2. Results and Discussion

2.1. Single Component Fmoc-Amino Acid Functionalised PiPrOx Systems

2.1.1. Polymer Synthesis and Functionalisation

Cationic ring opening polymerization (CROP) is a polymerization technique that provides good control over the molecular structure and a low polydispersity index (PDI) [15,16]. This polymerization technique was first reported in 1965 in a patent application [17] and it is receiving increasing interest thanks to the microwave-assisted CROP, a further improvement of this technique that was recently reported, which allows to shorten the polymerization time from hours to minutes [18,19].

The polymerisation procedure used is the same reported and optimized by Schubert and co-workers [20]. Briefly, propargyl-tosylate has been used as initiatior [21] to provide an alkyne group as the *α*-terminus functionality while the *ω*-terminus functionality, a hydroxyl group, was introduced by the terminator, water (Scheme 1). The ratio of monomer/initiatior used was 60:1, in dry AcN, and 4 M and 0.067 M were the concentration used, respectively. Matrix assisted laser desorption/ionization-time of flight (MALDI-TOF) of the purified polymers showed an average molecular weight of 5 kDa (n = 44) and a PDI of 1.1, as described in our previous work [12].

Scheme 1. Cationic ring opening polymerization (CROP) of 2-isopropyl-2-oxaoline. Propargyl-tosylate was used as initiator while water was used as terminator.

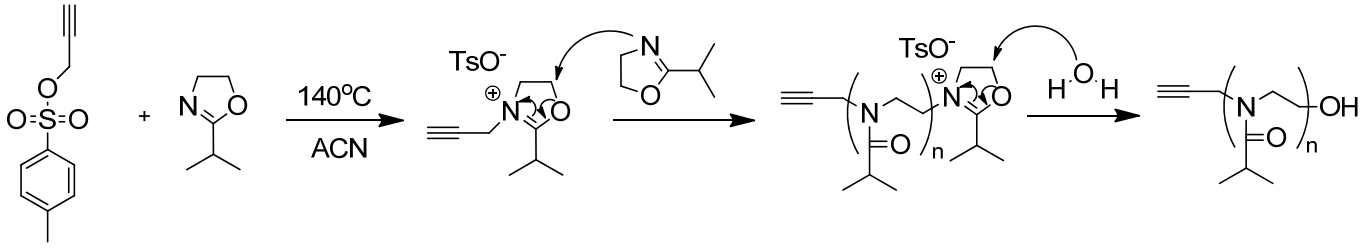

In order to explore the self-assembly behaviour and the influence that Fmoc-amino acids have when attached to PiPrOx chains, we decided to study a number of amino acids with different characteristics. These were previously reported Fmoc-*p*Y, Fmoc-Y, Fmoc-K complemented with Fmoc-F, which will in particular enable us to assess the relative importance of aromatic and electrostatic interactions in multicomponent self-assembly. Polymers functionalized with Fmoc-*p*Y (**1**) and Fmoc-K (**4**) (Scheme 2a) were attached through HBTU chemistry to a linker bearing an azide group and then clicked on the α-terminus of the polymer (Route A) (Scheme 2c). To avoid side reactions, Fmoc-K

side chain was protected with tert-butyloxycarbonyl (Boc) and deprotected prior to polymer functionalisation (Scheme 2b). Y functionalised PiPrOx (**2**) were obtained enzymatically by dephosphorylation of **1** (Route B) (Scheme 2d).

Scheme 2. (**a**) Synthetic strategy used to obtain Fmoc-phosphorylated tyrosine (Fmoc-*p*Y) and Fmoc-lysine (Fmoc-K) functionalised poly(2-isopropyl-2-oxazoline) (PiPrOx). (**a**) HBTU coupling used to functionalise the amino acid with 11-azido-3,6,9-trioxaundecan-1-amine; (**b**) Lysine side chain deprotection reaction with TFA; (**c**) Click reaction was used to functionalise PiPrOx with Fmoc-*p*Y-N_3 and Fmoc-K-N_3; (**d**) Dephosphorylation catalysed by alkaline phosphatase.

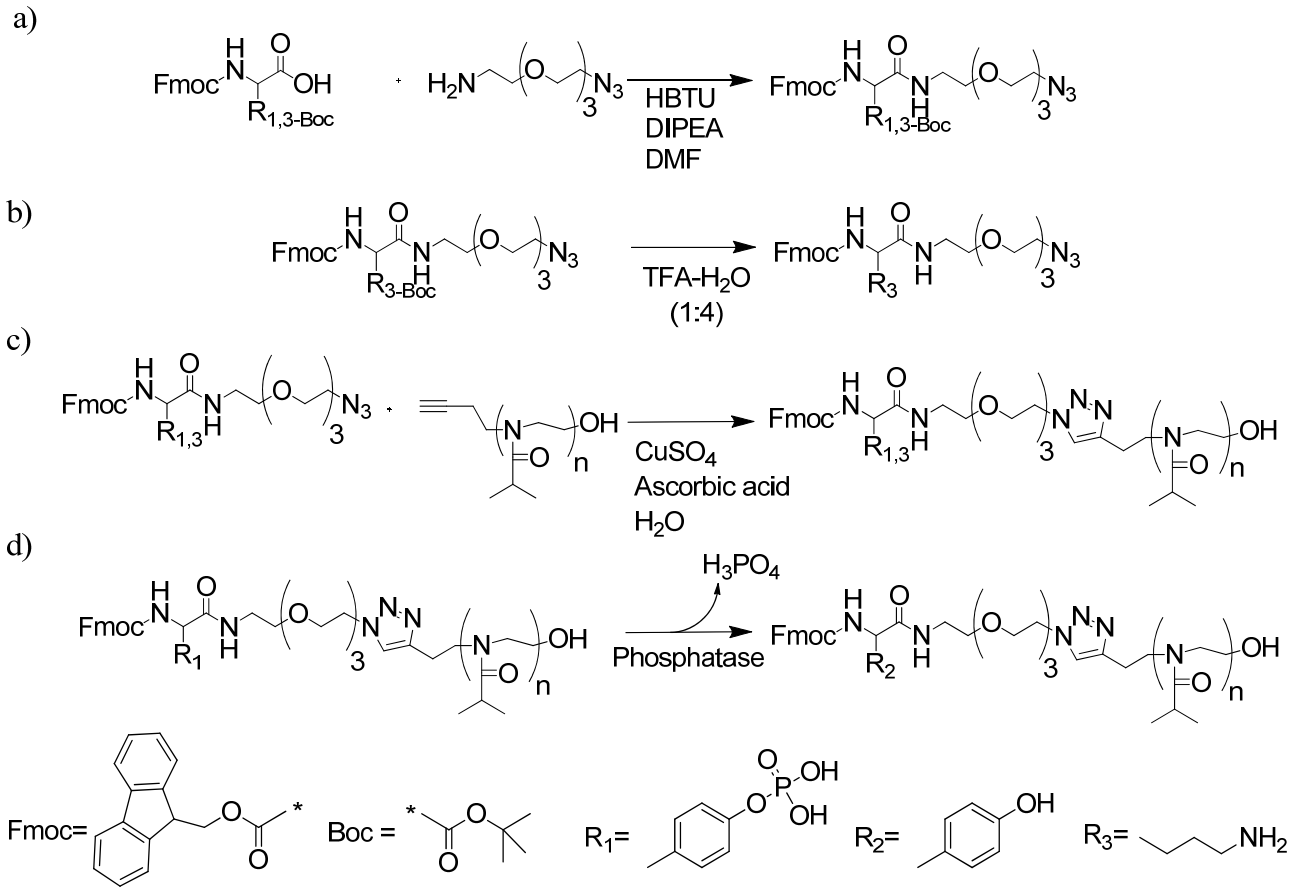

To obtain Fmoc-F functionalised PiPrOx (**3**) a different procedure was used since the click reaction gave poor yields (<30%), probably due to low solubility of Fmoc-F-N_3 complex in water. The inverted procedure was found to be successful (Route C) (Scheme 3). Briefly, the azide-containing linker was first clicked onto the polymer, then Fmoc-F was attached to the pendant free amine group through HBTU chemistry. The difference in thermal properties as a result of amino acid functionalisation was evident from turbidity measurements prior and after the click reaction. There is a difference of ~2 °C in the phase transition temperature between the unfunctionalised polymer (51 °C) and the polymer with the pendant amine group (53 °C) (ESI, Figure S1). The increased overall hydrophilicity of the polymer chains raises the LCST. This is due to the substitution of the alkyne group with the hydrophilic pendant amine group from 11-azido-3,6,9-trioxaundecan-1-amine, and it provides a first indication that the reaction was successful.

Scheme 3. Synthetic strategy used to obtain Fmoc-phenylanine (Fmoc-F) functionalised PiPrOx (Route B). (**a**) Click reaction was used to functionalise PiPrOx with 11-azido-3,6,9-trioxaundecan-1-amine; (**b**) HBTU chemistry was exploited to couple PiPrOx bearing the primary amino group at the α-terminus with Fmoc-F.

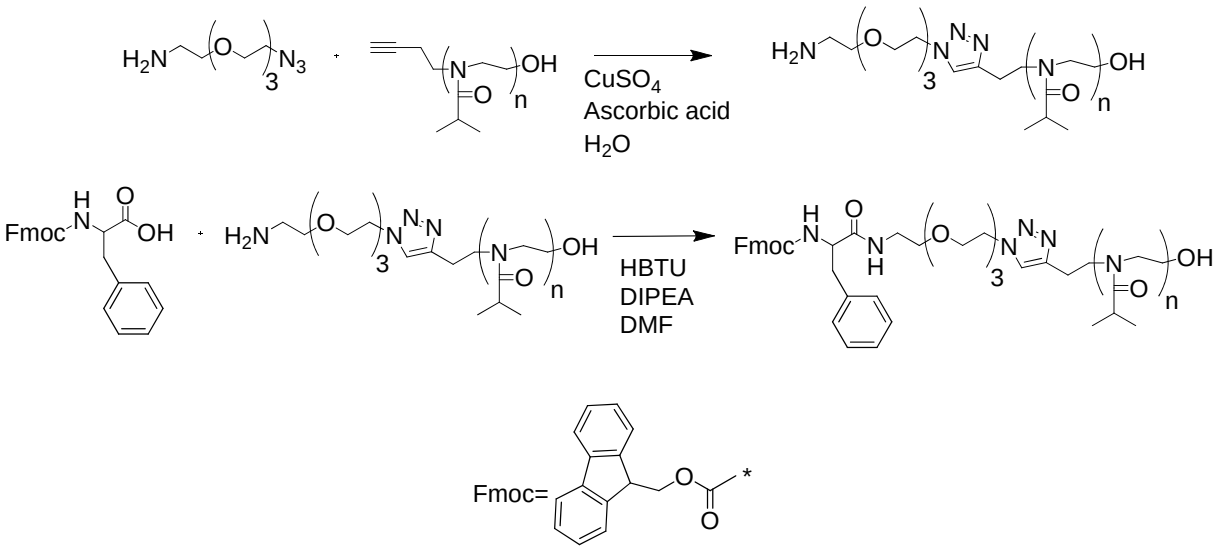

After attaching the Fmoc-amino acids, the loading was evaluated by exploiting the absorbance of Fmoc at 300 nm. Loading values are excellent in each case (>90%) (Table 2).

Attempts to functionalise PiPrOx with Fmoc-dipeptides using the same synthetic strategy were made, starting with Fmoc-F-*p*Y (**5**). Synthesis of Fmoc-F-*p*Y-N_3 complex was achieved through HBTU coupling (data not shown). Unfortunately, the loading yields achieved with Route A were low (~45%) despite several changes to the functionalisation strategy, e.g., substitution of solvent used for click reaction or altered reagent ratios. Route C gave even lower yields (~30%).

2.1.2. Phase Transition Temperature Studies

To assess if the polymer functionalisation affected the thermal properties of PiPrOx, we studied the thermal responsiveness of the polymers by measuring the transmittance by UV at 600 nm. The polymer concentration (1 mg/mL) was kept constant through all the UV experiments. Figure 1 gives a schematic representation of the conformation of the single component systems below and above the LCST, while Figure 3 shows the phase transition profiles of the polymers, *i.e.*, recorded transmittance against the temperature.

The phase transition temperature is contained within a range of 3 °C (37.7–40.7 °C) for **1**, **2** and **4**, while it drops to 31 °C for **3**. Their values are summarized in Table 1. There is a good correlation between the phase transition temperature found for each functionalized polymer and the hydrophobicity (LogP value) of amino acids (Table 1). The structural difference between **2** and **3** of a single hydroxyl group leads to a remarkable difference in the polymer behaviour. The presence of a charge on the amino acids K and *p*Y is expected to prevent close contact between residues, hampering the development of effective π-π stacking interactions between the Fmoc moieties. On the other hand, the presence of a hydrophobic residue, e.g., the phenyl functionality of phenylalanine, not only helps

the self-assembly process by increasing the overall hydrophobicity of the Fmoc-amino acid moiety but also improves the possibilities of interactions among amino acids/Fmoc moieties.

Figure 1. Schematic representation of self assembly behaviour of single component Fmoc-amino acid functionalised PiPrOx systems. (**a**) **1** forms unstable aggregates at room temperature but precipitates above the lower critical solution temperature (LCST) as shown for the unfunctionalised polymer; (**b**) **2** forms stable colloidal particles at room temperature which are kept when the temperature is increased; (**c**) **3** forms stable colloidal aggregates as seen for **2** both below and above the phase transition temperature; (**d**) **4** shows the same behaviour seen for the unfunctionalised polymer both at room temperature and above the LCST.

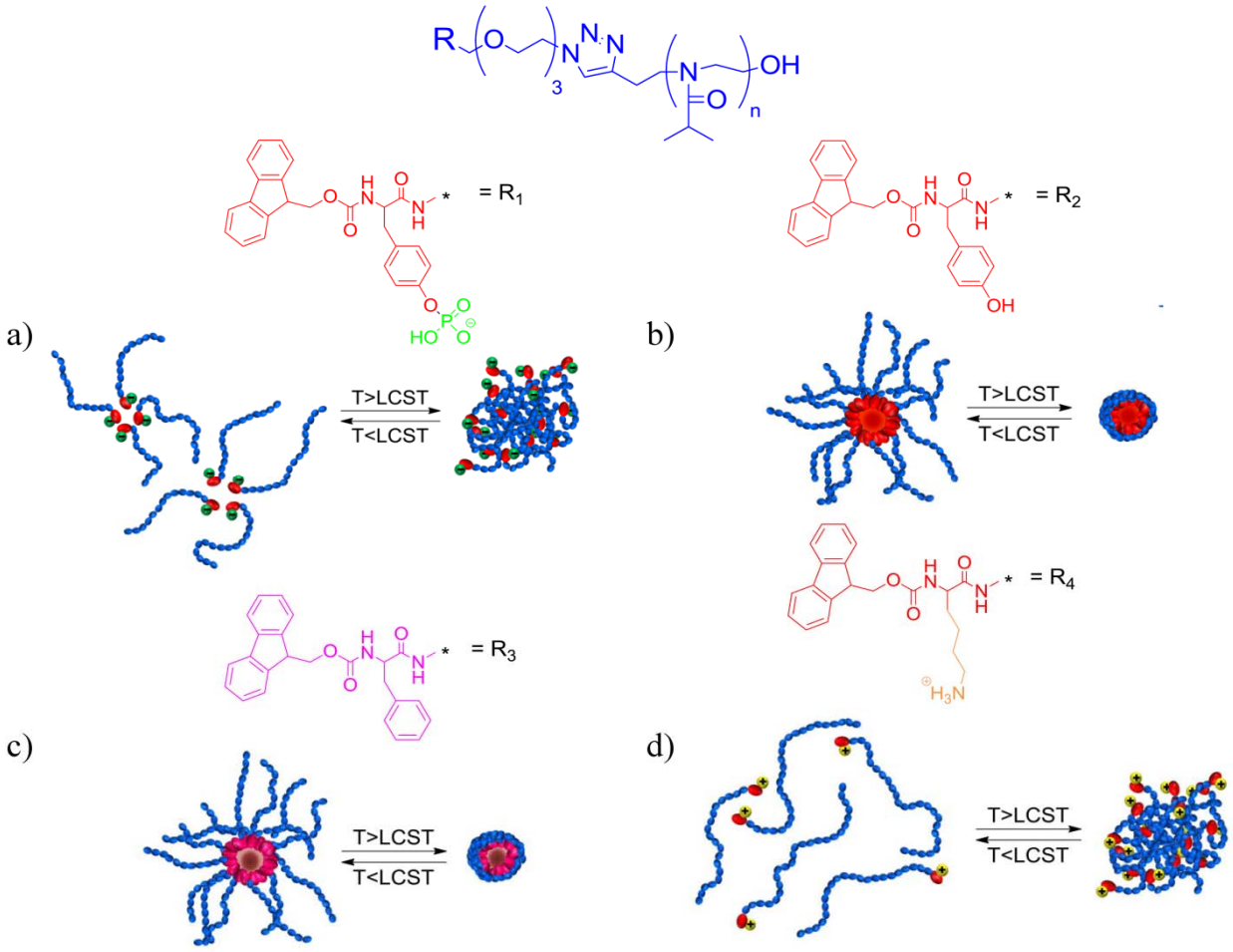

Table 1. Estimated LogP of the amino acids used to functionalise PiPrOx. *****Calculated LogP was assessed using ChemBioDraw chemical properties analysis tool.

Amino acid	CLogP*
*p*Y	−3.561
Y	−2.223
F	−1.556
K	−3.561

The differences in phase transition temperatures clearly show the substantial effects on the self-assembly behaviour upon end-functionalisation of polymer chains (Figure 2). The LCST of **5** (which was only partially functionalised) showed a sinusoid curve, starting to decrease at temperatures around 35 °C but reaching low transmittance values only close to the phase transition temperature of the unfunctionalised polymer (~51 °C) (Figure 2, inset). This data demonstrates that only fully functionalised polymers present a sharp phase transition.

Figure 2. Phase transition behaviour of unfunctionalised polymer (■), **1** (■), **2** (□), **3** (●), **4** (▲) and **5** (●) (inset). (Polymer concentration used = 1 mg/mL).

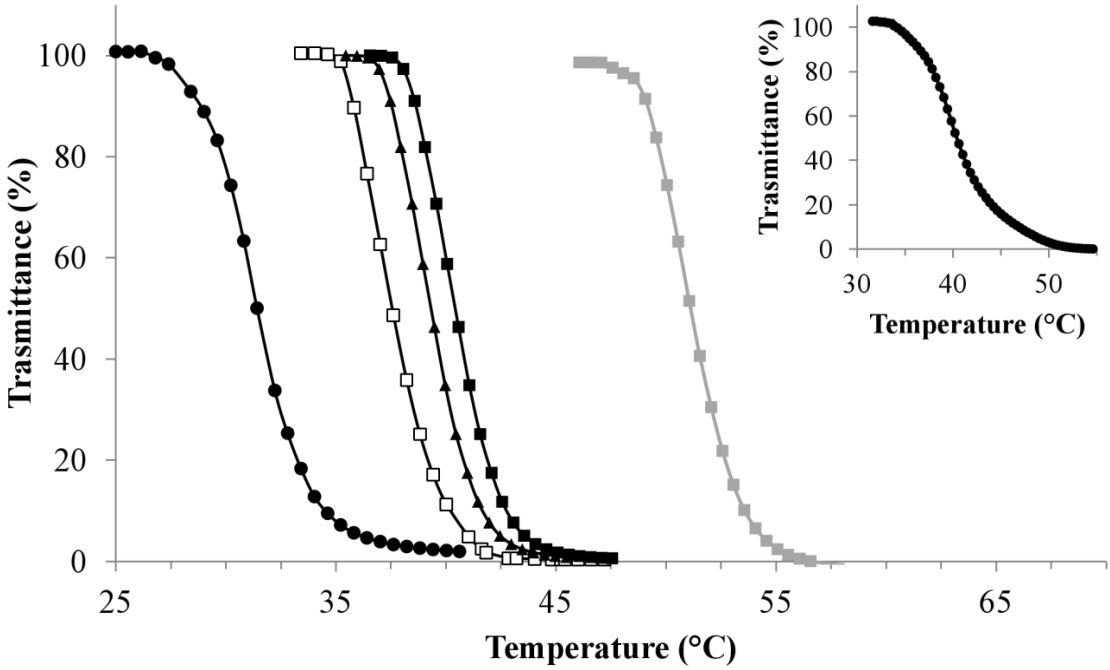

2.1.3. Dynamic Light Scattering Studies

Dynamic light scattering (DLS) was exploited to assess whether the functionalized polymer formed aggregates in solution (Figure 3). Solutions containing 2.5 mg/mL of polymer were dissolved in water and used to take the measurements. As previously reported, **1** forms aggregates, with an average particle size of 35 nm below the cloud point temperature, and precipitates when the temperature increases. **2** forms colloidal structures at room temperature (~90 nm) that resist when the phase transition temperature is reached. Above LCST the polymer chains collapse around the hydrophobic core formed by Fmoc-Y moieties and most likely colloidal aggregates are formed. Despite a substantial difference in phase transition temperature, **3** shows the same self-assembly behaviour observed for **2**, both above and below the cloud point temperature forming colloidal structures having an average particle size of 85 nm and 20 nm, respectively. **4** does not show self-assembly at room temperature while it precipitates above the phase transition temperature.

Figure 3. (**a**) Histogram showing the average hydrodynamic radius below (black columns) and above the cloud point temperature (grey columns); (**b**) Examples of dynamic light scattering (DLS) showing the hydrodynamic radius below (continuous line) and above (dotted line) the phase transition temperature of **4** (top) and **3** (bottom).

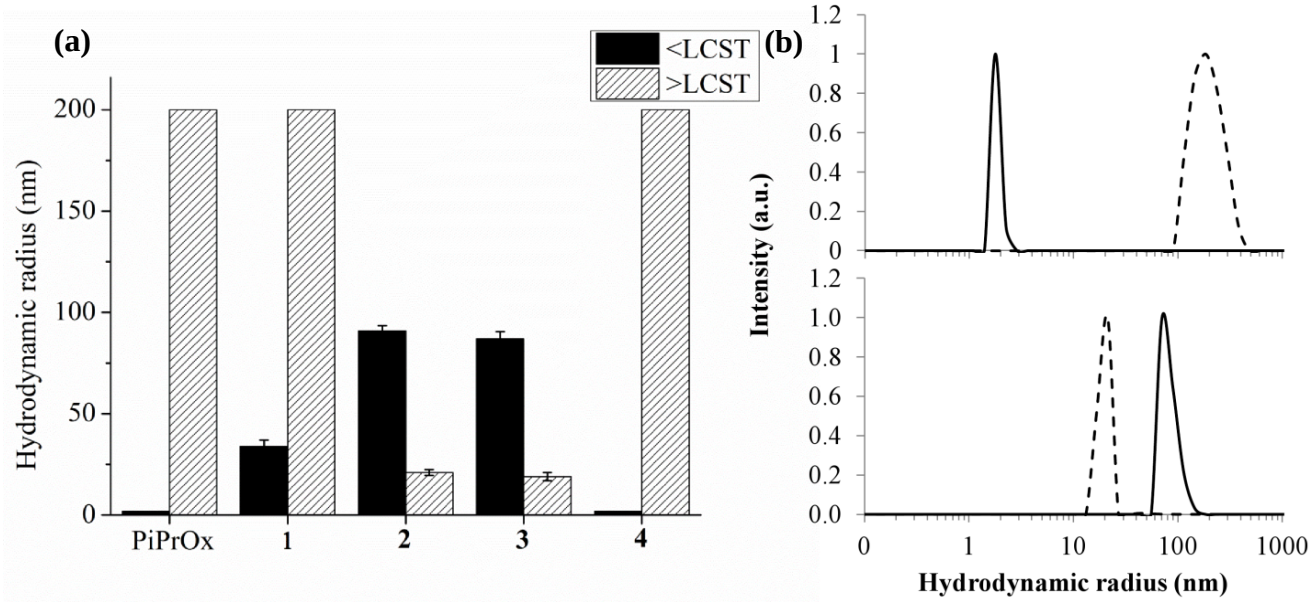

2.1.4. Critical Micelle Concentration Studies

To confirm the presence of aggregates suggested by DLS, we investigated the critical micelle concentration (CMC) exploiting the fluorescence properties of pyrene. It has been reported that the ratio between the first vibrational band (373 nm) and the third vibrational band (384 nm) (I/III) of pyrene is related to the hydrophobicity of the environment where the pyrene molecules are contained. The decrease of I/III ratio is dictated by a increase in the hydrophobicity of the environment [22–24].

A 0.25 mM stock solution of pyrene in methanol was prepared and further diluted 20 times. Concentrations of polymers ranging from 0.02 mM to 0.5 mM were dissolved in a constant volume of water (1 mL). 50 μL of the diluted pyrene solution was added to each sample and fluorescence was read using an excitation wavelength of 334 nm. Figure 4 shows the CMC of single component systems studied. The unfunctionalised polymer, in addition to **1** and **4** do not show a decrease in the I/III ratio, which give comparable values through the range of concentration studied. I/III ratio for **2** and **3** decreases with concentration forming a slope that was used to calculate the CMC, which is 0.20 mM and 0.21 mM for **2** and **3**, respectively. The similarity of the two values suggests that the nature of the colloidal structures formed is comparable. The initial and final I/III ratio agrees with values found in literature that indicate the presence of colloidal structures [8]. The shoulder at ~420 nm, which stays constant all through the experiments, is reported in literature as a semi-excimer [25], *i.e.*, when two pyrene molecules are only partially developing interactions.

Table 2 shows the characteristics of single component systems studied.

Figure 4. (**a**) Critical micelle concentration (CMC) of unfunctionalised polymer (■),**1** (■), **2** (□), **3** (●) and **4** (▲); Total volume of each sample 1.050 mL; (**b**) Example of pyrene spectra where no changes are observed upon increase of polymer concentration (**4**); (**c**) Example of pyrene spectra where I/III ratio decreases due to self-assembly (**3**).

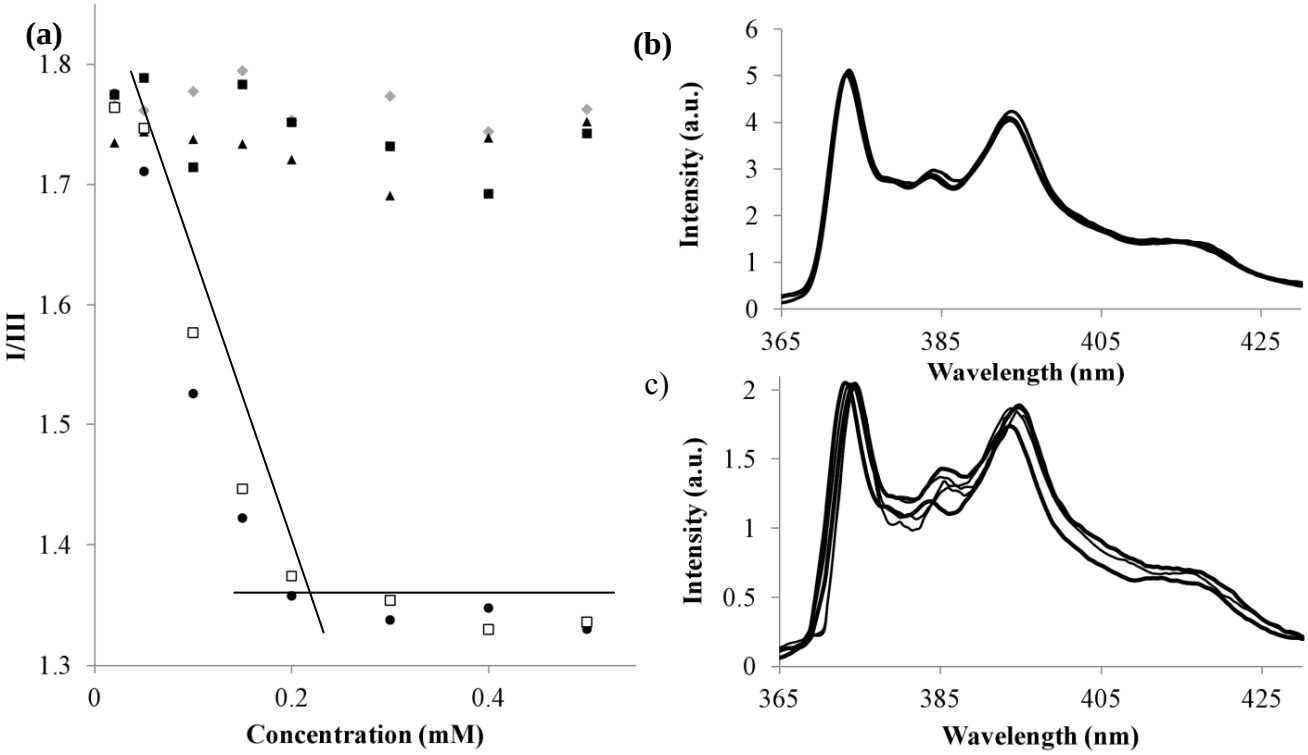

Table 2. Summary of characteristics of the single component systems studied.

Polymer	Functionalisation route	Functionalisation yield (%)	LCST (°C)	Radius (nm)		CMC (mM)
				<LCST	>LCST	
PiPrOx	/	/	51.5	1–2	>200	/
1	A	96	40.7	35–40	>200	/
2	B	/	37.7	80–90	15–20	0.21
3	A	94	31.4	75–85	15–20	0.20
4	C	93	39.2	1–2	>200	/

2.2. Two-Component Fmoc-Amino Acid Functionalised PiPrOx Systems

To provide further insight into the ability to produce multifunctional particle by mixing different functionalized polymers presented in Section 2, the enzyme responsive polymers (**1**) where mixed with **3** and **4**, to investigate how the self-assembly properties, triggered upon the catalytic action of phosphatase, were affected (**1** + **3** and **1** + **4**, followed by the addition of 5 μL of enzyme, give **2** + **3** and **2** + **4** (Figure 5)).

Figure 5. Schematic representation of self-assembly behaviour of dual component systems. (**a**) When **1** and **3** are mixed, only **3** undergoes self assembly, while, when **1** and **4** are mixed, both polymers self-assemble due to the contribution given by the opposite charges present on the amino acids; (**b**) Upon enzymatic dephosphorylation of the tyrosine, **2** and **3** form distinct colloidal aggregates despite their chemical similarity, while **4** is expelled from the nanostructures which are now formed only by **2**.

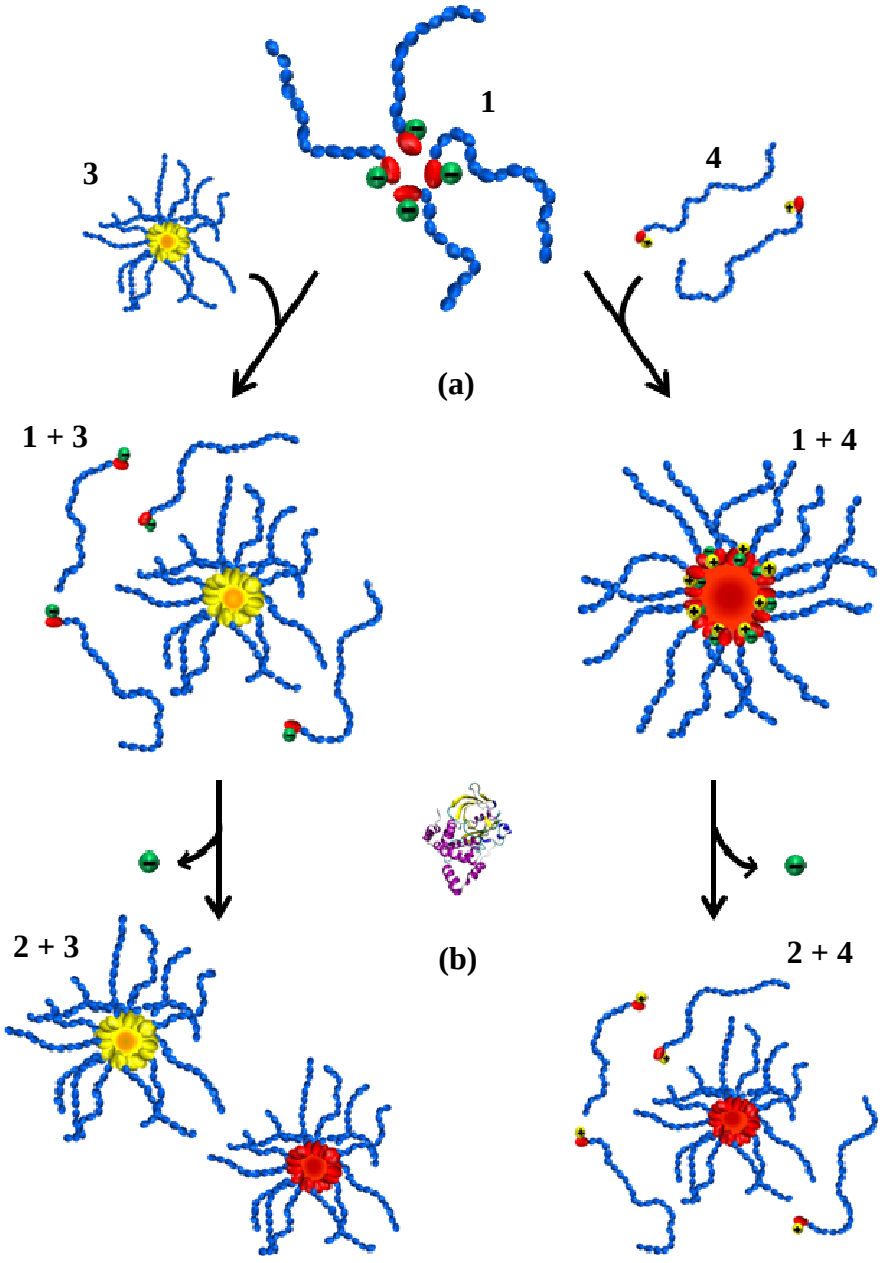

2.2.1. Phase Transition Temperature Studies

We proceeded to study phase transition profiles of the dual component systems to investigate how the cloud point temperature was affected. All the cloud point temperatures observed were found to be the average of the two phase transition temperatures of the single component systems studied in isolation. The total concentration was kept constant for all the turbidity measurements, *i.e.*, to achieve a 1 mg/mL concentration 0.5 mg of each polymer were dissolved in the solution. The cloud point

temperature was found to be 36.4 °C and 40.5 °C for the two-component systems before dephosphorylation (**1 + 3** and **1 + 4**, respectively), decreasing by roughly 2 °C after enzymatic reaction (Figure 6, Table 3). The decrease of the phase transition temperature implies that dephosphorylation is still taking place. Compared to the single component system, the phase transition profiles of all the two component systems studied is not as sharp. This behaviour can be explained by the difference in cloud point temperature of the different populations, in fact the slope is more broadened for the systems that have a higher difference in cloud point temperature (**1 + 3** and **2 + 3**). This theory agrees with the study reported by Gibson and co-workers [26], in which it was observed that when the phase transition temperature of a mixture of polymers is high curves are broadened and the cloud point temperature not as clear.

Figure 6. Phase transition profiles of **1 + 3** (■), **2 + 3** (□), **1 + 4** (●) and **2 + 4** (○). (Polymer concentration used = 1 mg/mL).

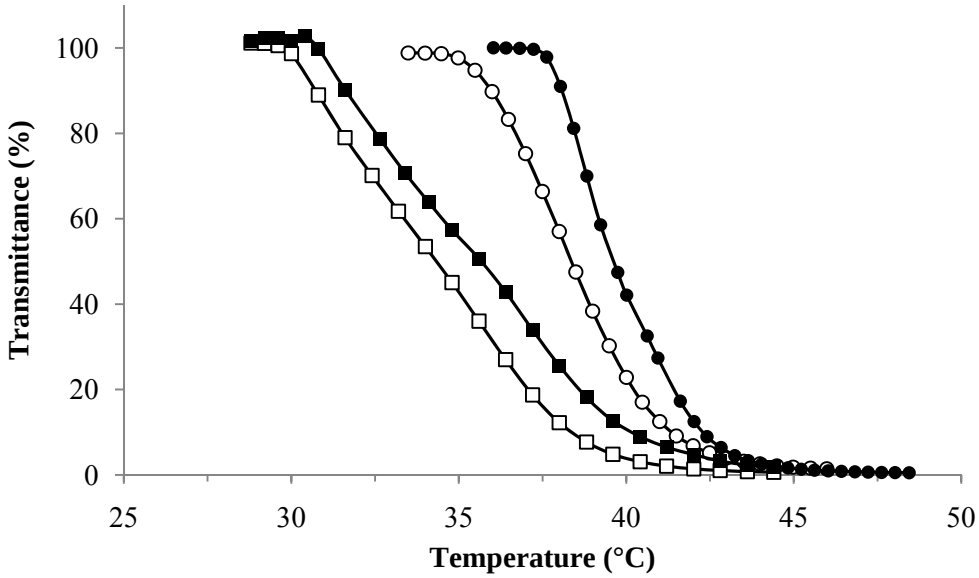

2.2.2. Dynamic Light Scattering Studies

DLS was used to assess whether the mixed polymers were forming colloidal structures (Figure 7). All systems investigated showed the presence of colloidal structures in the range of 90–135 nm at room temperature. This behaviour was expected for mixtures containing at least one population that undergoes self-assembly, *i.e.*, **1 + 3**, **2 + 3**, **2 + 4**, as shown in Paragraph 2. The self assembly behaviour of **1 + 4**, which gives large aggregates, is probably driven by the opposite charges present on the *p*Y and K side chains.

Above the phase transition temperature, the average particle size of all the systems decreases. In the case of **2 + 3** and **1 + 4** the precipitation of PiPrOx chains forming the corona-like structure contribute to form smaller colloidal aggregates having the core kept together by Fmoc-amino acid interactions. **1 + 3** and **2 + 4** have only one component forming aggregates while the population not taking part to structure formation is monodisperse in solution. Upon heating the **1** and **4** precipitate around the core formed by **3** and **2**, respectively, explaining the increased particle size above phase transition temperature.

Figure 7. (**a**) Average hydrodynamic radius below and above the cloud point temperature for two component systems; (**b**) Examples of DLS, showing the hydrodynamic radius below (continuous line) and above (dotted line) the phase transition temperature of two component systems.

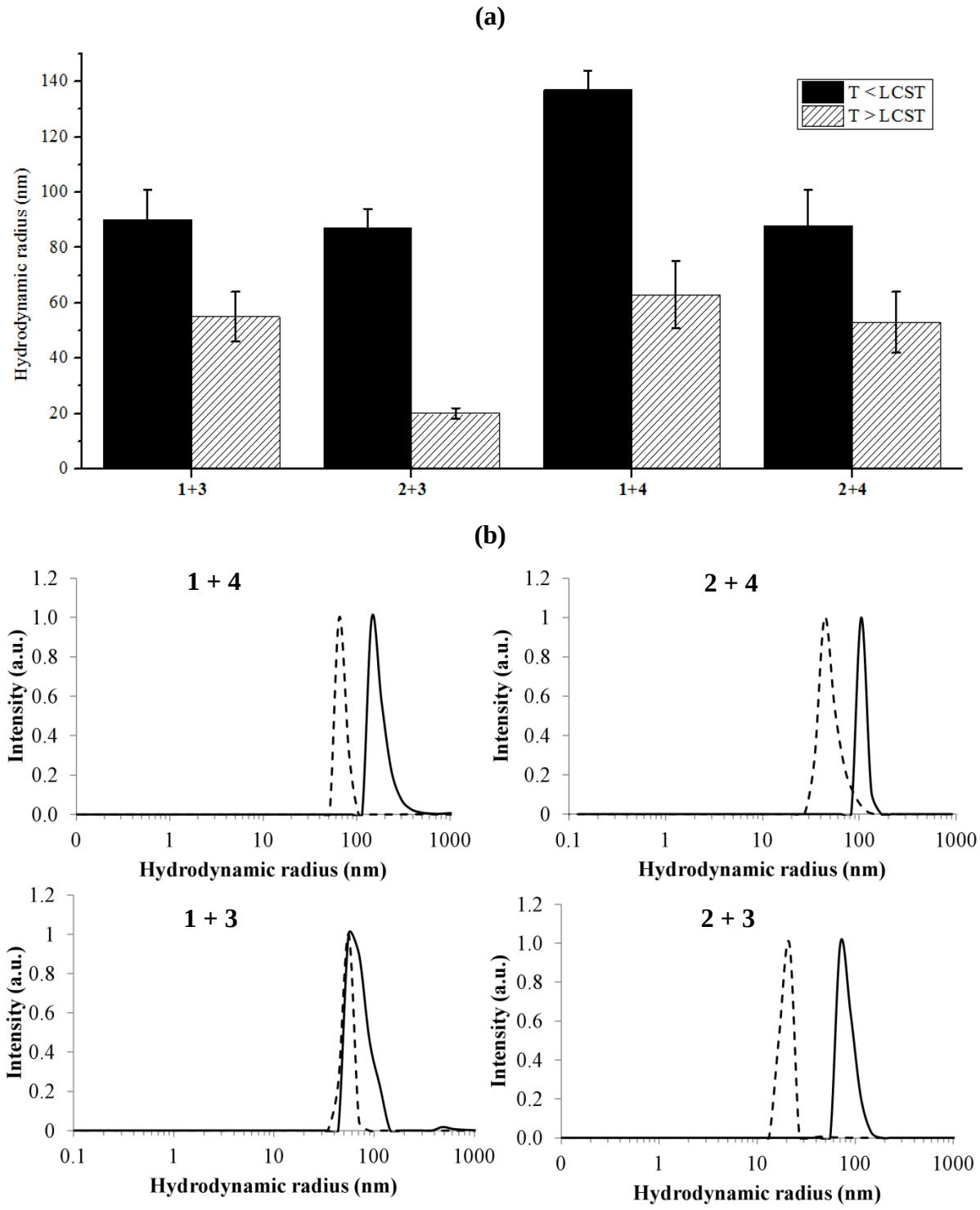

2.2.3. Critical Micelle Concentration Studies

The CMC was determined to provide insight into the structures of colloidal aggregates formed (Figure 8, Table 3). **2 + 3** has the lowest CMC value (0.20 mM) which is comparable to the value

obtained for **2** and **3** separately. **1 + 4** has a slightly higher CMC of 0.22 mM, which can be explained by the different nature of the interactions that lead to self-assembly and by the presence of the charges that make the environment inside the aggregates slightly less hydrophobic. The two remaining systems, **1 + 3** and **2 + 4** have a CMC profile which is almost identical, suggesting that only one of the two polymer populations is taking part to the aggregate structures since the CMC value (0.34 and 0.35 mM, respectively) is much higher than what found for **3** and **1** alone.

Figure 8. (**a**) CMC of **1 + 3** (■), **2 + 3** (□), **1 + 4** (●) and **2 + 4** (○); Total volume of each sample 1.050 mL; (**b**) Example of pyrene spectra where I/III ratio decreases at lower polymer concentrations (**2 + 3**); (**c**) Example of pyrene spectra where I/III ratio decreases at higher polymer concentrations (**1 + 3**). The CMC value was calculated as shown in Figure 4.

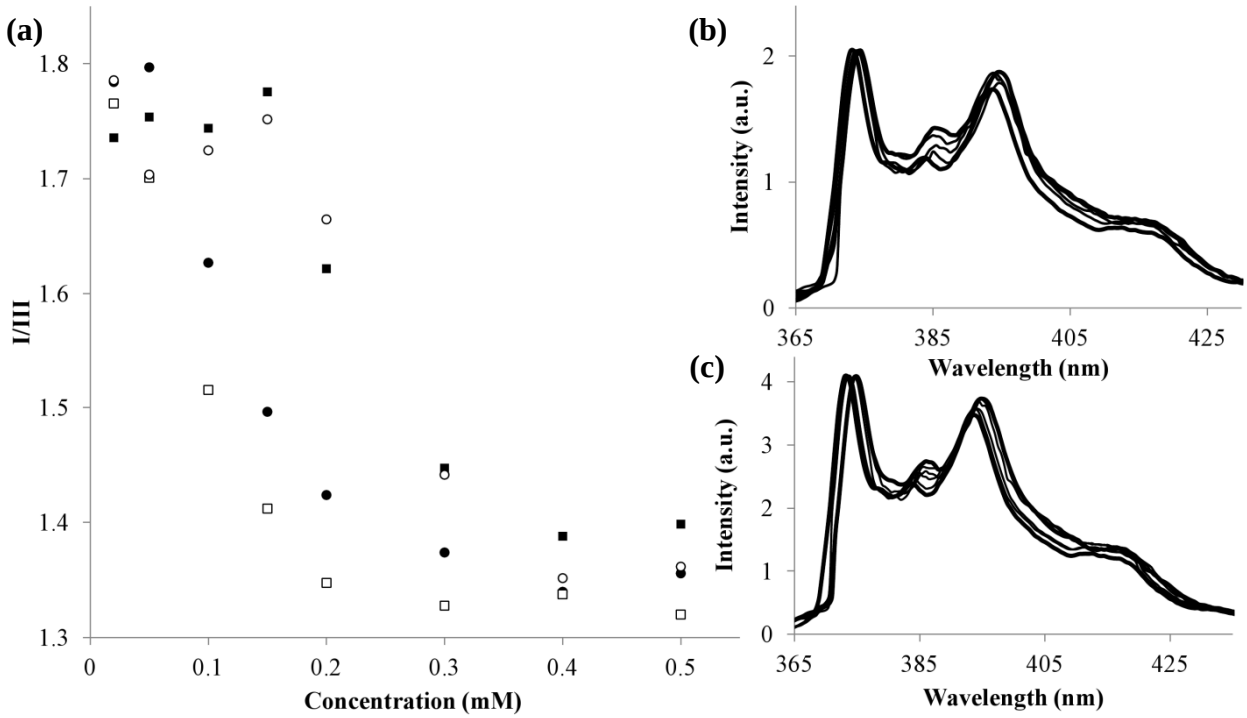

Table 3. Summary of characteristics of the dual component systems studied.

Polymer	LCST (°C)	Radius (nm)		CMC (mM)
		<LCST	>LCST	
1 + 3	36.4	91	56	0.35
2 + 3	36.6	89	20	0.20
1 + 4	40.3	136	63	0.22
2 + 4	38.8	92	53	0.34

3. Experimental Section

3.1. Materials

2-isopropyl-2-oxazoline (iPrOx, Tokyo Chemical Industry) was stirred overnight with calcium hydrade (CaH_2), vacuum distilled and stored under nitrogen atmosphere. Alkaline phosphatase (New

England BioLabs, 10.000 U/mL, one unit is defined as the amount of enzyme that hydrolyzes 1 μmol of pnitrophenylphosphate to *p*-nitrophenol in a total reaction volume of 1 mL in 1 mL at 37 °C), propargyl *p*-toluensulfonate (Fluka), 11-azido-3,6,9-trioxaundecan-1-amine (Aldrich), anhydrous *N,N*-dimethylformamide (DMF, Aldrich), *O*-(Benzotriazol-1-yl)-*N,N,N',N'*-tetramethyluronium hexafluorophosphate (HBTU, Aldrich), *N,N*-diisopropylethylamine (DIPEA, Aldrich), 3.5 kDa regenerated cellulose membrane (Triple Red Ltd), 500 Da cellulose acetate membrane (Aldrich), anhydrous acetonitrile (AcN, Aldrich), tetrahydrofuran (THF, Aldrich), fluorenylmethyloxycarbonyl-phosphorylated tyrosine (Fmoc-*p*Y-OH, Aldrich) Fmoc-lysine (tert-butyloxycarbonyl) (Fmoc-K(Boc)-OH, Aldrich), Fmoc-phenylalanine (Fmoc-F-OH, Aldrich) were used as received.

3.2. Instrumentation

Polymerization experiments were performed in a Biotage Initiator under constant heating mode. Fluorescence studies were performed on a Jasco FP-6500 spectrofluorometer. UV/Vis absorbance was measured on a Beckman Coulter DU 800 spectrophotometer equipped with a Beckman Coulter High Performance Temperature Controller. DLS was performed on an AVL/LSE-5004 light scattering electronics and multiple tau digital correlator using an angle of 90°. MALDI-TOF mass spectrometry was performed on a Kratos Analytical AXIIMA CFR using dithranol matrix. High performance liquid chromatography (HPLC) was carried out on a Dionex P680 HPLC system fitted with a UVD170U detector. An aliquot sample (100 μL) was injected into a Macherey-Nagel C18 column of the following dimensions: length 250 mm; internal diameter 4.6 mm; particle size 5 μm; flow rate 1 mL min^{-1}.

3.3. Polymer Synthesis

Polymerisation of iPrOx was performed following a procedure reported in literature [18,19]. Microwave vials (2.0–5.0 mL) were left in a heating oven (125 °C) and cooled down to room temperature under nitrogen atmosphere. A solution containing 0.067 M of propargyl p-toluensulfonate and 4 M of iPrOx was made directly in the microwave vial under nitrogen atmosphere and under stirring using dry AcN as the solvent. Total reaction volume was 3 mL. The vial was capped, and heated at 140 °C for 11 min. After the reaction, excess of H_2O was added to the vial, and the solution was extensively dialyzed against water for 3 days. After dialysis the solution was freeze-dried.

3.4. Synthesis and Characterisation of Fmoc-Amino Acids Bearing Terminal N_3

3.4.1. Fmoc-*p*Y-N_3

Synthesis of Fmoc-*p*Y bearing a terminal azide group was performed using a standard coupling procedure. The carboxylic terminus of Fmoc-*p*Y was activated using 2 equiv of HBTU and DIPEA in DMF/DCM (1:1). A DMF/DCM (1:1) solution containing 1 equiv of 11-azido-3,6,9-trioxaundecan-1-amine was added to the activated the amino acid**.** The reaction lasted overnight under stirring. The dialysis, which was followed by freeze-drying, was performed with a membrane of regenerated cellulose (500 Da molecular weight cut off). The purity of the obtained

compound after the purification process was assessed by HPLC (initial flow rate 40% H_2O, 60% AcN) dissolving 0.2 mg of Fmoc-*p*Y-OH in 1 mL of AcN/H_2O (1:1 ratio), as a control experiment, and the same amount of Fmoc-*p*Y-N_3 complex (Figure S2).

3.4.2. Fmoc-K-N_3

Synthesis of Fmoc-K(Boc)-OH bearing a terminal azide group was performed using the same standard coupling procedure used for Fmoc-*p*Y-N_3. Removal of Boc protecting group was performed using a solution of TFA/H_2O (1:4 ratio). The reaction lasted overnight and the solvents were eliminated using a vacuum pump. A cycle of dialysis and freeze drying followed. The purity of the obtained compound after the purification process was assessed by HPLC (initial flow rate 40% H_2O, 60% AcN) dissolving 0.2 mg of Fmoc-K(Boc)-OH in 1 mL of AcN/H_2O (1:1 ratio) , as a control experiment, and the same amount of Fmoc-K(Boc)-N_3 complex (Figure S3). After deprotection the Fmoc-K-N_3 was analyzed through MS to check the reaction was successful (Figure S4).

3.4.3. "Click" Reaction

Azide-alkyne cycloaddition was performed in water, using $CuSO_4$ as catalyst and ascorbic acid as reducing agent to convert Cu (II) in Cu (I). The ratio used is the following: propargyl/azide/$CuSO_4$ 1:2:0.3. 2 equiv of azide and 0.3 equiv of $CuSO_4$ and ascorbic acid were dissolved in an aqueous solution containing the polymer (final volume 7 mL). The reaction was left overnight under stirring, before going through the purification process, using a membrane having a molecular weight cut off of 3.5 kDa. The freeze-dried polymer was used to evaluate the Fmoc loading by UV absorbance of Fmoc at 300 nm, comparing it with the concentration/absorbance dependence of a calibration curve. Different calibration curves were calculated for each amino acid. The calibration curves were obtained taking the absorbance values of Fmoc-*p*Y-OH and Fmoc-K-OH dissolved in H_2O, at different concentrations. A known amount of polymer (~0.5–1.0 mg) was dissolved in 1 mL of water. The obtained absorbance at 300 nm was used to evaluate the concentration of Fmoc.

4. Conclusions

We report a modular approach to achieve compartmental systems that can be selectively triggered upon catalytic action of phosphatase, achieving reconfiguration of the nanostructures formed. Functionalising PiPrOx with different Fmoc-amino acids enables the control of morphology and temperature responsiveness of self-assembly tailoring the dimensions of the formed structure. We studied four different amino acids having different characteristics that drastically influence the self-assembly behaviour of the system, which charge complementarity providing a means to produce mixed systems while aromatic systems were thought to self-separate into distinct populations. As shown, amino acids provide a powerful toolbox and the characteristics provided by other amino acids still remain to be explored.

The straightforward synthetic strategy used, combined with the advantages provided by the Fmoc molecule, makes this system useful to build a platform that can be used for systematic studies on modular compartmental systems. Fmoc has been used for its self-assembly and fluorescence properties

but we envisage that it could be replace by a more biocompatible aromatic functionality still able to develop interesting self-assembly interactions through π-π stacking, e.g., fully peptidic self-assembly moieties [27]. The development of such a system could lead to application in the drug delivery field due to the low cytotoxicity profiles showed by POx family [28–30] and the "switchability" introduced by enzyme catalysis.

References

1. Grzybowski, B.A.; Wilmer, C.E.; Kim, J.; Browne, K.; Bishop, K.J.M. Self-assembly: From crystals to cells. *Soft Matter* **2009**, *5*, 1110–1128.
2. Zayed, J.M.; Nouvel, N.; Rauwald, U.; Scherman, O.A. Chemical complexity—Supramolecular self-assembly of synthetic and biological building blocks in water. *Chem. Soc. Rev.* **2010**, *39*, 2806–2816.
3. Börner, H.J.; Kühnle, H.; Hentschel, J. Making "smart polymers" smarter: Modern concepts to regulate functions in polymer science. *J. Polym. Sci.* **2010**, *48*, 1–14.
4. Löwik, D.W.P.M.; Leunissen, E.H.P.; van den Heuvel, M.; Hansen, M.B.; van Hest, J.C.M. Stimulus responsive peptide based materials. *Chem. Soc. Rev.* **2010**, *39*, 3394–3412.
5. Ulijn, R.V. Enzyme-responsive materials: A new class of smart biomaterials. *J. Mater. Chem.* **2006**, *16*, 2217–2225.
6. Cohen Stuart, M.A.; Huck, W.T.S.; Genzer, J.; Müller, M.; Ober, C.; Stamm, M.; Sukhorukov, G.B.; Szleifer, I.; Tsukruk, V.V.; Urban, M.; Winnik, F.; Zauscher, S.; Luzinov, I.; Minko, S. Emerging applications of stimuli-responsive polymer materials. *Nat. Mater.* **2010**, *9*, 101–113.
7. Torchilin, V.P. Structure and design of polymeric surfactant-based drug delivery systems. *J. Control. Release* **2001**, *73*, 137–172.
8. Amir, R.J.; Zhong, S.; Pochan, D.J.; Hawker, C.J. Enzymatically triggered self assembly of block copolymers. *J. Am. Chem. Soc.* **2009**, *131*, 13949–13952.
9. Kühnle, H.; Börner, H.G. Biotransformation on polymer—Peptide conjugates: A versatile tool to trigger microstructure formation. *Angew. Chem. Int. Ed.* **2009**, *48*, 6431–6434.
10. Ku, T.H.; Chen, M.P.; Thompson, M.P.; Sinkovits, R.S.; Olson, N.H.; Baker, T.S.; Gianneschi, N.C. Controlling and switching the morphology of micellar nanoparticles with enzymes. *J. Am. Chem. Soc.* **2011**, *133*, 8392–8395.
11. Wang, C.; Chen, Q.; Wang, Z.; Zhang, X. An enzyme-responsive polymeric superamphiphile. *Angew. Chem. Int. Ed.* **2010**, *49*, 8612–8615.
12. Caponi, P.F.; Qiu, X.P.; Vilela, F.; Winnik, F.M.; Ulijn, R.V. Phosphatase/temperature responsive poly(2-isopropyl-2-oxazoline). *Polym. Chem.* **2011**, *2*, 306–308.
13. Yang, Z.M.; Gu, H.W.; Fu, D.G.; Gao, P.; Lam, J.K.; Xu, B. Enzymatic formation of supramolecular hydrogels. *Adv. Mater.* **2004**, *16*, 1440–1444.
14. Caponi, P.F.; Winnik, F.M.; Ulijn, R.V. Charge complementary enzymatic reconfigurable polymeric nanostructures. *Soft Matter* **2012**, *8*, 5127–5130.
15. Aoi, K.; Okada, M. Polymerization of oxazolines. *Prog. Polym. Sci.* **1996**, *21*, 151–208.
16. Hoogenboom, R.; Schlaad, H. Bioinspired poly(2-oxazoline)s. *Polymers* **2011**, *3*, 467–488.

17. Allied Chemical Corporation. Carbon-Nitrogen Backbone Chain Polymers. U.S. Patent 3,483,141, 9 December 1969.
18. Wiesbrock, F.; Hoogenboom, R.; Abeln, C.H.; Schubert, U.S. Single-mode microwave ovens as new reaction devices: Accelerating the living polymerization of 2-ethyl-2-oxazoline. *Macromol. Rapid Commun.* **2004**, *25*, 1895–1899.
19. Wiesbrock, F.; Hoogenboom, R.; Leenen, M.A.M.; Meier, M.A.R.; Schubert, U.S. Investigation of the living cationic ring-opening polymerization of 2-methyl-, 2-ethyl-, 2-nonyl-, and 2-phenyl-2-oxazoline in a single-mode microwave reactor. *Macromolecules* **2005**, *38*, 5025–5034.
20. Hoogenboom, R.; Wiesbrock, F.; Huang, H.; Leenen, M.A.A.; Thijs, H.M.L.; van Nispen, S.F.G.M.; van der Loop, M.; Fustin, C.A.; Jonas, A.M.; Gohy, J. F.; Schubert, U.S. Microwave-assisted cationic ring-opening polymerization of 2-oxazolines: A powerful method for the synthesis of amphiphilic triblock copolymers. *Macromolecules* **2006**, *39*, 4719–4725.
21. Fijten, M.W.M.; Haensch, C.; van Lankvelt, B.M.; Hoogenboom, R.; Schubert, U.S. Clickable poly(2-Oxazoline)s as versatile building blocks. *Macromol. Chem. Phys.* **2008**, *209*, 1887–1895.
22. Kalyanasundaram, K.; Thomas, J.K. Environmental effects on vibronic band intensities in pyrene monomer fluorescence and their application in studies of micellar systems. *J. Am. Chem. Soc.* **1977**, *99*, 2039–2044.
23. Konuk, R.; Cornelisse, J.; McGlynn, S.P. Fluorescence quenching of pyrene by Cu^{2+} and Co^{2+} in sodium dodecyl sulfate micelles. *J. Phys. Chem.* **1989**, *93*, 7405–7409.
24. Chaudhuri, A.; Haldar, S.; Chattopadhyay, A. Organization and dynamics in micellar structural transition monitored by pyrene fluorescence. *Biochem. Biophys. Res. Commun.* **2009**, *390*, 728–732.
25. Yamazaki, I.; Winnik, F.M.; Winnik, M.A.; Tazuke, S. Excimer formatlon in pyrene labeled hydroxypropyl cellulose in water: Picosecond fluorescence studies. *J. Phys. Chem.* **1987**, *91*, 4213–4216.
26. Ieong, N.S.; Hasan, M.; Phillips, D.J.; Saaka, Y.; O'Reilly, R.K.; Gibson, M.I. Polymers with molecular weight dependent LCSTs are essential for cooperative behaviour. *Polym. Chem.* **2012**, *3*, 794–799.
27. Zhao, X.; Pan, F.; Xu, H.; Yaseen, M.; Shan, H.; Hauser, C.A.E.; Zhang, S.; Lu, J.R. Molecular self-assembly and applications of designer peptide amphiphiles. *Chem. Soc. Rev.* **2010**, *39*, 3480–3498.
28. Goddard, P.; Hutchinson, L.E.; Brown, J.; Brookman, L.J. Soluble polymeric carriers for drug delivery. Part 2. Preparation and *in vivo* behaviour of *N*-acylethylenimine copolymers. *J. Control. Release* **1989**, *10*, 5–16.
29. Woodle, M.C.; Engbers, C.M.; Zalipsky, S. New amphipatic polymer-lipid conjugates forming long-circulating reticuloendothelial system-evading liposomes. *Bioconjugate Chem.* **1994**, *5*, 493–496.
30. Zalipsky, S.; Hansen, C.B.; Oaks, J.M.; Allen, T.M. Evaluation of blood clearance rates and biodistribution of poly(2-oxazoline)-grafted liposomes. *J. Pharm. Sci.* **1996**, *85*, 133–137.

© 2012 by the authors; licensee MDPI, Basel, Switzerland. This article is an open access article distributed under the terms and conditions of the Creative Commons Attribution license (http://creativecommons.org/licenses/by/3.0/).